Journal of Nuclear Medicine, published on April 30, 2021 as doi:10.2967/jnumed.120.260034

Cerenkov luminescence imaging in prostate cancer: not the only light that shines

Judith olde Heuvel[1,2], Berlinda J. de Wit-van der Veen[1], Henk G. van der Poel[3], Pim J. van Leeuwen[3], Elise M. Bekers[4], Maarten R. Grootendorst[5], Kunal N. Vyas[5], Cornelis H. Slump[2], Marcel P.M. Stokkel[1]

[1]Department of Nuclear Medicine, Netherlands Cancer Institute, Amsterdam, The Netherlands.

[2]Technical Medical Centre, University of Twente, Enschede, The Netherlands

[3]Department of Urology, Netherlands Cancer Institute, Amsterdam, The Netherlands.

[4]Department of Pathology, Netherlands Cancer Institute, Amsterdam, The Netherlands.

[5]Lightpoint Medical Ltd., Chesham, United Kingdom

Corresponding author: B.J. de Wit-van der Veen – l.vd.veen@nki.nl – Plesmanlaan 121, 1066 CX Amsterdam – Tel:+3120512 7882 – Fax:+31205122290

First author: J. olde Heuvel – j.olde.heuvel@nki.nl – Plesmanlaan 121, 1066 CX Amsterdam – Tel:+3120512 7843 – Fax:+31205122290 (PhD-student)

Words:4990

This research is supported by KWF Kankerbestrijding and Technology Foundation STW (Grant number 15175).

Short running title: CLI: Not the only light that shines

ABSTRACT

Introduction. Cerenkov luminescence imaging (CLI) is a novel imaging technology that might have the ability to assess surgical margins intra-operatively during prostatectomy using Gallium-68 prostate-specific membrane antigen ([^{68}Ga]Ga-PSMA-11). This study evaluates the accuracy of CLI compared to histopathology and as exploratory objective investigates the characteristics of the identified chemiluminescence signal.

Materials and Methods. After intravenous injection of a mean ^{68}Ga-PSMA-11 activity of 69MBq intraoperatively, all excised specimens were imaged with CLI. Areas of increased signal were marked for histopathological comparison and scored for likelihood of being a positive surgical margin (PSM) using a 5-point Likert scale. In addition, the chemiluminescence signal was investigated in three radioactive and three non-radioactive specimens using CLI.

Results. In 15 patients, the agreement between CLI and histopathology was 60%; this improved to 83% when including close surgical margins (≤1mm). In six hotspots, CLI correctly identified PSMs on histopathology, located at the apex and mid-prostate. In all 15 patients an increased signal at the prostate base was observed, without the presence of the primary tumor in this area in eight patients. This chemiluminescence signal was also observed in non-radioactive prostate specimens, with a half-life of 48±11min. The chemiluminescence hampered the visual interpretation of four PSMs at the base.

Conclusion. CLI is able to correctly identify margin status, including close margins, in 83% of the cases. The presence of a diathermy-induced chemiluminescent signal hampered image interpretation, especially at the base of the prostate. In the current form, CLI is most applicable to detect PSMs and close margins in the apex and mid-prostate.

Keywords. Cerenkov luminescence imaging, prostate cancer, 68-Gallium-PSMA, intra-operative assessment, surgical margins

INTRODUCTION

Positive surgical margins (PSMs) on histopathology occur in 11-38% of the patients undergoing a radical prostatectomy(*1*,*2*). These men have a higher risk of receiving adjuvant local radiotherapy(*1*,*3*). Multiple intra-operative margin assessment technologies are developed that aim to enable a radical excision(*4*). Of these, NeuroSAFE is currently the only method used for clinical decision making with good diagnostic accuracy (sensitivity: 93.5% & specificity: 98.8%)(*5*), but the procedure is labor intensive, time consuming and costly and prone to sampling errors and therefore only used in a small number of centers(*6*). In addition, a study showed that 70% of the secondary resections due to a PSM on NeuroSAFE did not contain tumor(*7*).

A recently introduced technology to aid intra-operative margin assessment is Cerenkov luminescence imaging (CLI)(*8–12*). Cerenkov radiation is induced when a charged particle travels faster than the velocity of light in the tissue, thus polarizing the tissue. When the locally polarized medium returns to its ground state, Cerenkov photons are emitted(*10*). Tumor-specific tracers, like ^{68}Gallium prostate-specific-membrane antigen ([^{68}Ga]Ga-PSMA-11), induce Cerenkov radiation and the detected rays from superficial layers can guide towards areas with high suspicion of a PSM. Recent studies on this application have already shown the feasibility and safety of this technique(*13*,*14*).

During radical prostatectomy, electrosurgery (i.e. diathermy) is used for cutting and coagulation of tissue. This technique uses radio-frequency currents to increase the intracellular temperature, which in turn can result in vaporization and blood clotting. A preclinical study suggested that heat may induce chemiluminescence with wavelengths between 400-710nm(*15*,*16*), which overlap with the Cerenkov spectrum (400-1000nm)(*9*). Thus, this chemiluminescence might interfere with the CLI signal, indicating a potential limitation(*15*,*16*). However, these studies were conducted with animal tissue and used other thermal sources, thus the spectrum, half-life and other features in human perfused tissue after diathermy application are unknown.

In our prior study the technical feasibility of ^{68}Ga-PSMA-11 CLI for margin assessment was assessed in a small population with prostate cancer (PCa)(*14*). This consecutive study evaluates the accuracy of CLI compared to histopathology in a larger population, and as a explorative objective investigates the characteristics of a chemiluminescent signal observed on CLI.

MATERIALS AND METHODS

The present study was approved by the local Ethics Committee (NL8256, trialregister.nl) and all subjects signed written informed consent. High-risk primary PCa patients scheduled for robot-assisted radical prostatectomy were enrolled. The inclusion criteria were biopsy proven prostate cancer with a tumor lesion ≥1.5cm on MRI and a PSMA-positive intra-prostatic lesion on PSMA PET/CT (^{18}F-DCFPyL or ^{68}Ga-PSMA-11). The exclusion criterion was the use of Indocyanine green during surgery (not standard of care), since this may influence CLI measurements. In all patients, CLI was not used for surgical or histopathological decision making.

Surgery and Intra-operative CLI

An intravenous injection of ~100MBq [^{68}Ga]Ga-HBED-CC-PSMA (ABX GmbH, Radeberg, Germany) was given after docking the daVinci® surgical system. Immediately after prostatectomy, *ex vivo* Cerenkov images of the prostate specimen were acquired with the LightPath® system (Lightpoint Medical Ltd, Chesham, UK) using the following imaging parameters: exposure time of 150s, 8×8 pixel binning (pixel resolution 938µm), no optical filter. A 550nm shortpass filter was applied when areas of increased signal (called "hotspots") were visualized on non-filtered images.

Understanding the Characteristics of the Chemiluminescent signal

Effect of Urine Contamination on CLI. Since ^{68}Ga-PSMA-11 undergoes renal clearance, it was verified if radioactive urine might affect CLI, by first imaging three specimens without rinsing from potential blood and urine contamination. Subsequently, it was rinsed twice with 500mL 0.9% sodium chloride (NaCl) and imaged again. The visual and quantitative difference between the images were compared. In the other patients, CLI was performed after rinsing the prostate once with 500mL of 0.9% NaCl.

CLI and Flexible Autoradiography (FAR) of Non-radioactive Prostate Specimens. The prostate specimens of three patients undergoing prostatectomy without injection of ^{68}Ga-PSMA-11 (the 'non-radioactive specimens') were imaged with CLI to investigate the characteristics of the chemiluminescence signal. On these images multiple regions of interest were drawn to quantify any chemiluminescence signal and the reduction in this signal by applying a 550nm shortpass filter (application of 800nm shortpass filter in Supplemental Fig. 1). The half-life of chemiluminescence was determined by consecutive imaging over ~60 minutes.

To investigate an alternative imaging method that is potentially less susceptible to chemiluminescence than CLI, flexible autoradiography (FAR) was used on non-radioactive specimens. A 12µm flexible scintillating film (Lightpoint Medical Ltd. and Scintacor Ltd., UK) was draped over the specimen, and as a whole this was imaged within the LightPath system, thus discarding the need to development a scintillating film. The opaque nature of the scintillator may block some of the chemiluminescent photons while detecting the positrons emitted by ^{68}Ga-PSMA-11(*17*). The reduction in chemiluminescent signal from photon absorption by the FAR was assessed, as well as the half-life over a ~60 minute measurement period.

FAR on ^{68}Ga-PSMA-11 Containing Prostate Specimens. In three CLI patients, FAR was used on ^{68}Ga-PSMA-11 containing prostate specimens in addition to CLI imaging. Images with and without 550nm shortpass filter were acquired to investigate the effect of the FAR on the signal originating from ^{68}Ga-PSMA-11 uptake and in relation to chemiluminescence.

Histopathology

After CLI acquisitions, the specimens were send for standard histopathological examination by an experienced uropathologist (EMB). A PSM was defined as cancer extending into the inked surface in accordance with the guidelines(*18*). At the marked locations the tumor-to-margin distance was measured.

Image Analysis

Image quantification and processing was performed in MATLAB R2017b (The MathWorks, Natick, USA) as previously described(*14*). The mean radiance (photons/s/cm^2/steradian) was measured in areas showing 'hotspots' (suspected tumor) and in areas with no increased signal (tissue background), the signal-to-tissue background ratios (SBRs) were calculated. Hotspots were defined as all signals higher than 3 times the standard deviation (sd) of the empty background(*19*). Visual interpretation of all images was performed post-operatively by two independent readers (JoH, LdWvdV). All hotspots were scored to assess the likelihood of such a spot actually being a PSM using a 5-point Likert scale (1 – most likely negative surgical margin (NSM), 5 – most likely PSM). Features used to interpret hotspots were: knowledge of the tumor location on PSMA PET/CT, size of the hotspot (required size ≥1mm due to 8×8 binning), intensity above tissue background, and usage of diathermy. Observers were blinded for each other's scores and histopathology; any disagreement was settled in consensus. A score on the Likert scale (LS) of 4 and 5 was considered PSM in further analysis, 1-3 as NSM. The extent of the PSMs was measured on CLI images

(longest axis) and compared to the extent measured on histopathology. Agreement between the margin status on histopathology and CLI was assessed in three areas of the prostate: base (top 1cm), mid-gland and apex (bottom 1cm). The agreement was calculated with and without additional scoring (using the LS), and with and without inclusion of a close surgical margin (CSM≤1mm tumor to margin distance).

RESULTS

Results Intra-operative CLI Radioactive Specimens

In this study 17 patients were included. One patient had to be excluded due to an unsuccessful ^{68}Ga-PSMA-11 labelling on the day of the surgery and one due to the use of Indocyanine green, leaving 15 patients to be included in the analysis. The mean injected activity was 69±27MBq (range 23-121MBq), with on average 70±15min (range 44-105min) between injection and CLI acquisition. The patient and procedure characteristics can be found in Table 1.

Fig. 1 displays examples of CLI images showing hotspots identified as PSM, NSM or CSM on histopathology. The overall agreement between CLI ('hotspot') and histopathology with respect to the margin status (PSM or NSM) was 31% without further Likert scoring by users (Fig. 2 & Supplemental Table 1). This overall agreement improved to 59% when ≤1mm margins (CSM) on histopathology were also classified as positive. Discordance between CLI and histopathology was mainly present at the prostate base.

Additionally, all hotspots on CLI were interpreted using the 5-point Likert score (LS) by the independent users. A disagreement between readers occurred in eight hotspots, and concordance was settled in consensus. In all these cases, the disagreement concerned 4 versus 5, or 1 versus 2-3. With the addition of the Likert score, overall agreement between CLI and histopathology was 60%, which improved to 83% with inclusion of CSM. Ten hotspots were actually identified as histopathological confirmed PSM (Table 2); six were detected at the apex/mid-prostate with a LS ≥4 (true positive), and four were detected at the base with a LS of 3 (false negative). There were no proven PSMs that did not show signal on CLI. The extent of PSM measured on CLI and histopathology showed in 5/10 PSMs a difference of less than 1mm, Table 2.

The average±sd SBR of PSM was 7.1±3.5, CSM was SBR:5.0±1.9 and for NSM this was 5.8±3.9 on a non-filtered image, Fig. 3.

In all 15 patients, an intense signal was observed on CLI at the prostate base, Fig. 3. In eight of these patients the tumor was not located in the base, as indicated on pre-operative PET/CT. These findings indicate the presence of an additional chemiluminescence signal, which may explain the high false negative rate at the base.

Understanding the Characteristics of the Chemiluminescent Signal

Effect of Urine Contamination on CLI. After rinsing once, the chemiluminescence signal at the base was reduced to 93% of the original CLI-signal (Supplemental Fig.2). After the second rinsing, the signal decreased to 88% compared to the unrinsed prostate. Time between the rinsed images and unrinsed image was respectively 5 and 10 minutes.

CLI and FAR of Non-radioactive Prostate Specimens. The chemiluminescent signal was also visible on CLI images from three 'non-radioactive specimens', primarily at the base, Fig. 4. This observation underlines the hypothesis that chemiluminescence is not originating from ^{68}Ga-PSMA-11. The SBR of the chemiluminescence was 4.9±1.1 on the unfiltered image. The half-life without an optical filter was 48±11min, and 52±16min with the 550nm filter. The application of a 550nm shortpass filter resulted in a reduction to 15% of the original chemiluminescence signal, which was comparable to the CLI signal reduction by filtering in radioactive specimens (18%). The application of FAR resulted in the reduction of the chemiluminescent signal to 60% of the original CLI image, both with and without 550nm filtering, Fig. 5.

FAR on ^{68}Ga-PSMA-11 Containing Prostate Specimens. FAR put on the radioactive specimens reduced the chemiluminescence to 70% at locations where diathermy was applied. Whereas tumor and tissue background signals were amplified by FAR on average 3.2 times the original signal (Fig. 5 and Supplemental Fig.3).

DISCUSSION

The primary aim of the current study was to assess the concordance in margin status between intra-operative CLI and post-operative histopathology. This study showed that agreement between CLI and histopathology ranged from 31-83% depending on definition of PSM and addition of by Likert score. The explorative aim of the study was to characterize the observed chemiluminescence. It was concluded that this signal is unrelated to ^{68}Ga-PSMA-11, has a mean SBR of 4.9±1.1 and a half-life of 48±11 minutes. This chemiluminescence indeed proved clinically relevant as it hampered easy identification of 4/10 PSMs on CLI, all four located at the base.

When considering the histopathological PSM definition as tumor on ink, the false positive rate found in the current study was considered high; with 24/30 hotspots (LS≥4) not having a PSM on histopathology (agreement 31%). Comparable false positive rates are also described by Darr *et al.*, though their workflow and CLI protocol is slightly different(*13*). Several explanations for these false-positives findings can be considered. Firstly, in 19 false positives the tumor-to-margin distance was within 1mm on histopathology. Due to the average positron range of 2.8mm for ^{68}Ga(*20*), the CLI technique has inherent difficulties in the detection of PSM defined as 'tumor on ink'. If instead of tumor on ink a PSM is defined as a margin of ≤1mm, agreement between CLI and histopathology increases to 83%. The clinical relevance of a CSM is contradicting; some argue that having a CSM results in a higher rate of biochemical recurrence compared to a NSM, though it is not an independent predictor(*21*). The role of a CSM in biochemical recurrence is found by Izard *et al*. as well, though having a CSM definition of <0.1mm(*22*). CLI might have added value to guide surgeons toward areas with an increased risks on PSM and CSM. The positron range might as well influence the correlation between the extent of the PSM on CLI and histopathology; in 5/10 PSMs the deviation between the extent on CLI and histopathology was more than 1mm (Table 2). This can as well be caused by shrinkage of the specimen during fixation and histopathological processing. Still, it is worth further exploring, as the extent of a PSM is an important prognostic factor(*23*).

Secondly, the presence of the chemiluminescence signal also contributed to the false positive findings, especially in the base. In all included patients chemiluminescence was visible in the base in varying degrees, even when the primary tumor was not located there, and it was observed in non-radioactive specimens as well. The latter proved that this signal does not originate from ^{68}Ga-PSMA-11. Extensive rinsing with sodium chloride did not make the signal disappear, thus eliminating the effect of radioactive urine and blood contamination, as was initially

suggested by Darr *et al.*(*13*). Our hypothesis is that this signal is chemiluminescence, caused by the use of diathermy. The sudden heat from electro surgery, is known to result in the production of Reactive Oxygen Species(*24*). After a cascade of reactions, decomposition of the molecule occurs resulting in emission of optical photons. These photons partially overlap with the Cerenkov spectrum(*9,13,14*). In our institute, diathermy is mainly performed when separating the prostate from the bladder, though it is also used in other areas. Therefore, chemiluminescence is most prevalent at the base, explaining why the correspondence between CLI (hotspot yes/no) and histopathology was only 20% (Fig.2). Despite the fact that the addition of image interpretation with a Likert score improved agreement, four PSMs at the base were false negative on CLI with a LS of 3, Fig. 3C. To facilitate better detectability of PSMs a method to distinguish between Cerenkov and the diathermy-induced chemiluminescence is eminent.

The mean SBR of the chemiluminescent signal and PSM-suspected hotspots on unfiltered images were comparable: 4.9±1.1 and 5.3±2.3, respectively, Fig. 3. In 550nm filtered images the SBR of the PSM was larger 9.9±5.5 then chemiluminescent 4.2±0.3, though they still overlap. Next, filtered images are more susceptible to noise resulting in high SBRs. A study by Spinelli *et al.* found a heat-induced chemiluminescent half-life of 4-6 minutes in chicken breast tissue(*15*). They suggested a potential distinction between Cerenkov and chemiluminescence based on half-life. However, the half-life's of both signals in prostatic tissue showed large overlap; chemiluminescence half-life was 48±11 minutes compared to 68 minutes for ^{68}Ga. The discrepancy in chemiluminescence half-life compared with Spinelli *et al.* may be explained by the differences in tissue composition and methods used to induce thermal damage. A focused ultrasound transducer (60Watt) was used by Spinelli *et al*. (*15*), while in our institution a monopolar diathermy device (Intuitive, Sunnyvale, CA) at 40Watt was used.

Another solution may be to look for alternative forms for monopolar diathermy, with a lower wattage resulting in less thermal induction and spread(*25*,*26*), for example the PEAK PlasmaBlade (Medtronic, USA). Next, a theoretical method to reduce the presence of free radicals in tissue, thereby preventing lipid peroxidation, might be the use of anti-oxidants like vitamin-C or E(*27*) or to investigate the influence of rapid cooling. Whether these are viable solutions requires further investigation and for clinical use it is of key importance that they do not interfere with the surgical outcome or histopathological evaluation of the specimens.

FAR, an opaque film that largely blocks optical photons while positrons are detected directly, was used to investigate if this is less susceptible to chemiluminescence as CLI. The signal originating from ^{68}Ga-PSMA-11

containing areas (tumor and benign) were enhanced ~3.2 times, compared to these areas on CLI (Fig. 5 & Supplemental Fig.3), whereas chemiluminescence was reduced to 70%. Although this technique might help to distinguish between ^{68}Ga-PSMA-11 and chemiluminescence, there are some practical drawbacks to consider. Firstly, the FAR obscures the white light image, so the anatomical and spatial information of the specimen is absent. Secondly, accurate positioning of the FAR onto the specimen proved challenging, and more work is needed to improve its ease of use. Thirdly, the FAR does not block all optical photons originating from the chemiluminescence, Fig. 5. Finally, contamination of the scintillator might lead to false positive hotspots, Fig. 5.

Future Perspectives on CLI

The current histopathological definition of a PSM, being tumor on ink, is a requirement that currently cannot be met with ^{68}Ga-PSMA-CLI. Therefore, instead of being used as a stand-alone technology our group proposes CLI as screening tool for using NeuroSAFE. By sending only areas that show suspicious hotspots on Cerenkov images for pathological examination, instead of the entire neurovascular bundle, the procedure may become far more efficient (Supplemental Fig.4). 60-75% of the PSMs occur at the apex or posterolateral side of the prostate (*23*,*28*), while the chemiluminescence occurs especially at the base. When diathermy is used in other prostate area's the surgeons are able to identify these locations visually, so inclusion of this knowledge during image interpretation may further improve the accuracy of CLI for combined use with NeuroSAFE.

CONCLUSION

CLI of ^{68}Ga-PSMA-11 can be used for margin assessment during prostatectomy. In the current study agreement between CLI and histopathology was 31-83% for the entire prostate, depending on definition of PSM and application of image interpretation using the Likert scale. The best results were achieved for cancer ≤1mm from the margin on histopathology. The presence of chemiluminescence from diathermy, especially profound in the basal area, hampers accurate image interpretation of CLI. Therefore, ^{68}Ga-PSMA-11 CLI is most applicable to detect close and positive surgical margins in the apex and posterolateral side.

Compliance with Ethical Standards

Funding. This research is supported by KWF Kankerbestrijding and Technology Foundation STW, as part of their joint strategic research programme 'Technology for Oncology' (Grant number 15175).

Conflict of Interest. KNV and MRG are employees of and have equity interest in Lightpoint Medical Ltd. The other authors do not have any conflicts of interest to disclose.

KEY POINTS

QUESTION: Can CLI be used to detect positive surgical margins intra-operatively in prostate cancer surgery?

PERTINENT FINDINGS: In this clinical trial of 15 patients, CLI was able to detect positive surgical margins and tumor close to the surface (≤1mm). Still, the presence of diathermy-induced chemiluminescence hampers the application in its current form.

IMPLICATIONS FOR PATIENT CARE: CLI showed potential as intra-operative method to find tumor close to the surface, however, the influence of a chemiluminescent artifact on the CLI images should be reduced prior to clinical implementation.

REFERENCES

1. Yossepowitch O, Briganti A, Eastham JA, et al. Positive surgical margins after radical prostatectomy: a systematic review and Contemporary update. *Eur Urol*.2014;65:303-313.

2. Stephenson AJ, Wood DP, Kattan MW, et al. Location, extent and number of positive surgical margins do not improve accuracy of predicting prostate cancer recurrence after radical prostatectomy. *J Urol*.2009;182:1357-1363.

3. Silberstein J, Eastham J. Significance and management of positive surgical margins at the time of radical prostatectomy. *Indian J Urol*.2014;30:423-428.

4. olde Heuvel J, de Wit-van der Veen BJ, Huizing DMV, et al. State-of-the-art intraoperative imaging technologies for prostate margin assessment: a systematic review. *Eur Urol Focus*.2020 [Epub ahead of print].

5. Schlomm T, Tennstedt P, Huxhold C, et al. Neurovascular structure-adjacent frozen-section examination (NeuroSAFE) increases nerve-sparing frequency and reduces positive surgical margins in open and robot-assisted laparoscopic radical prostatectomy: experience after 11,069 consecutive patients. *Eur Urol*.2012;62:333-340.

6. Dinneen EP, Van Der Slot M, Adasonla K, et al. Intraoperative frozen section for margin evaluation during radical prostatectomy: a systematic review. *Eur Urol Focus*.2019;6:664-673.

7. van der Slot MA, Bakker MA, Klaver S, et al. Intraoperative assessment and reporting of radical prostatectomy specimens to guide nerve-sparing surgery in prostate cancer patients (NeuroSAFE). *Histopathology*.2020;77:539-547.

8. Grootendorst MR, Cariati M, Pinder SE, et al. Intraoperative assessment of tumor resection margins in breast-conserving surgery using 18 F-FDG Cerenkov luminescence imaging: a first-in-human feasibility study. *J Nucl Med*.2017;58:891-898.

9. Ciarrocchi E, Belcari N. Cerenkov luminescence imaging: physics principles and potential applications in

biomedical sciences. *EJNMMI Phys*.2017;4:14.

10. Robertson R, Germanos MS, Li C, Mitchell GS, Cherry SR, Silva MD. Optical imaging of Cerenkov light generation from positron-emitting radiotracers. *Phys Med Biol*.2009;54:N355-365.

11. Tanha K, Pashazadeh AM, Pogue BW. Review of biomedical Čerenkov luminescence imaging applications. Biomed Opt Express.2015;6:3053.

12. Thorek DLJ, Riedl CC, Grimm J. Clinical Cerenkov Luminescence Imaging of ^{18}F-FDG. J Nucl Med.2014;55:95-98.

13. Darr C, Harke N, Radtke JP, et al. Intraoperative 68Gallium-PSMA Cerenkov luminescence imaging for surgical margins in radical prostatectomy – a feasibility study . *J Nucl Med*.2020;61:1500-1506.

14. olde Heuvel J, de Wit-van der Veen BJ, van der Poel HG, et al. 68Ga-PSMA Cerenkov luminescence imaging in primary prostate cancer: first-in-man series. *Eur J Nucl Med Mol Imaging*.2020;47:2624–2632

15. Spinelli AE. Weak light emission of soft tissues induced by heating. *J Biomed Opt*.2018;23:046003.

16. Boschi F, Basso PR, Corridori I, et al. Weak biophoton emission after laser surgery application in soft tissues: Analysis of the optical features. *J Biophotonics*.2019;12:e201800260.

17. Vyas KN, Grootendorst M, Mertzanidou T, et al. Flexible scintillator autoradiography for tumor margin inspection using 18F-FDG. *Proc. SPIE* 10478.2018:1047811.

18. Samaratunga H, Montironi R, True L, et al. International society of urological pathology(ISUP) consensus conference on handling and staging of radical prostatectomy specimens. Working group 1: specimen handling. *Mod Pathol*.2011;24:6-15.

19. Pukelsheim F. The three sigma rule. *Am Stat*.1994;48:88-91.

20. Moses WW. Fundamental limits of spatial resolution in PET. *Nucl Instruments Methods Phys Res Sect A*. 2011;648:S236-S240.

21. Herforth C, Stroup SP, Chen Z, et al. Radical prostatectomy and the effect of close surgical margins: results

from the shared equal access regional cancer hospital (SEARCH) database. *BJU Int*.2018;122:592-598.

22. Izard JP, True LD, May P, et al. Prostate cancer that is within 0.1 mm of the surgical margin of a radical prostatectomy predicts greater likelihood of recurrence. *Am J Surg Pathol*.2014;38:333-338.

23. Koskas Y, Lannes F, Branger N, et al. Extent of positive surgical margins following radical prostatectomy: Impact on biochemical recurrence with long-term follow-up. *BMC Urol*.2019;19:1-8.

24. Kobayashi K, Okabe H, Kawano S, Hidaka Y, Hara K. Biophoton Emission Induced by Heat Shock. *PLoS One*.2014;9:e105700.

25. Lyons SD, Law KSK. Laparoscopic vessel sealing technologies. *J Minim Invasive Gynecol*.2013;20:301-307.

26. Hefermehl LJ, Largo RA, Hermanns T, Poyet C, Sulser T, Eberli D. Lateral temperature spread of monopolar, bipolar and ultrasonic instruments for robot-assisted laparoscopic surgery. *BJU Int*.2014;114:245-252.

27. Catala A. Lipid peroxidation. In: Repetto M, Semprine J, Boveris A. *Lipid Peroxidation: Chemical Mechanism, Biological Implications and Analytical Determination*. IntechOpen,2012:3-30.

28. Eastham JA, Kuroiwa K, Ohori M, et al. Prognostic significance of location of positive margins in radical prostatectomy specimens. *Urology*.2007;70:965-969.

TABLE 1. Patient demographics, TNM classification, tumor characteristics, TBR on pre-operative PET/CT-scan, and information regarding CLI imaging.

Patient No.	Age (y)	TNM pre-operative	TNM post-operative	PSA (µg/L)	Gleason Score pre-operative biopsy	TBR on PSMA PET	Intra-operative injected activity (MBq)	Time between injection and CLI imaging hh:mm	Estimated* activity in prostate at start CLI-imaging (kBq)
1	67	cT3bN0M0	pT3aN0R1	29.9	4+4=8	4.9	118.0	01:35	111
2	71	cT2bN0M0	pT3aN0R1	4.4	4+4=8	8.1	68.4	01:04	93
3	58	cT1cN0M0	pT2cN0R0	5.3	4+4=8	1.8	88.1	01:25	26
4	73	cT3bN1M0	pT3bN1R0	8.3	4+5=9	8.9	75.6	00:59	92
5	66	cT3bN0M0	pT3bN0R0	2.7	4+4=8	2.1	96.7	01:00	52
6	63	cT2aN0M0	pT2N0R0	6.4	4+5=9	3.8	64.6	01:02	37
7	55	cT2cN0M0	pT3aN1R0	9.3	4+4=8	3.7	62.1	01:14	61
8	48	cT3bN1M0	pT3bN1R1	4.4	4+5=9	4.4	23.4	01:05	48
9	73	cT2cN0M0	PT3aN0R0	5.6	4+3=7	2.7	44.7	00:44	26
10	69	cT3aN0M0	pT3aN0R1	65	4+5=9	2.4	47.9	00:56	151
11	72	cT2bN0M0	pT3bN1R0	8.7	4+4=8	2.8	47.6	01:05	42
12	76	cT1cN0M0	pT2N0R1	9.2	3+4=7	2.5	65.4	01:02	69
13	65	cT2cN0M0	pT3aN0R1	5.1	4+3=7	1.7	121.1	01:26	8
14	67	cT2bN0M0	pT3bN0R1	18.6	4+5=9	3.7	37.4	01:14	14
15	74	cT1cN0M0	pT2cN0R0	7.9	4+4=8	3.5	70.2	01:45	33

*Estimation made based on uptake on preoperative PET imaging, uptake in prostate as %injected activity, TBR=tumor-to-background ratio. TNM classification according to American Joint Committee on Cancer Cancer Staging Manual. c=clinical, p=pathological, T=tumor, N=node, M=metastasis**.** R0=negative surgical margin, R1=positive surgical margin.

TABLE 2. Overview of the histopathology and CLI results from the ten histopathological PSMs.

Ptn no.	Location of PSM on histopathology	Likert score	SBR CLI	Gleason score at the PSM	Extent PSM histopathology (mm)	Extent PSM CLI (mm)
1	Apex right	5	13.2	8	3	6.9
2	Apex left	5	5.9	8	4	4.3
8	Base central	3	7.1	10	14	14
	Base left	3	6.1	10	14	12
	Apex right	5	8.7	10	15	12
	Base right	3	6.1	9	10	9.6
10	Base central	3	5.1	8	9.0	6.7
12	Apex posterior/ mid-prostate	5	2.8	3+4=7	6.0	6.5
13	Apex left	5	2.9	8	1.0	1.4
14	Apex posterior /mid-prostate	5	12.3	10	2.0	12.0

* PSM=positive surgical margin, SBR=signal-to-tissue background ratio

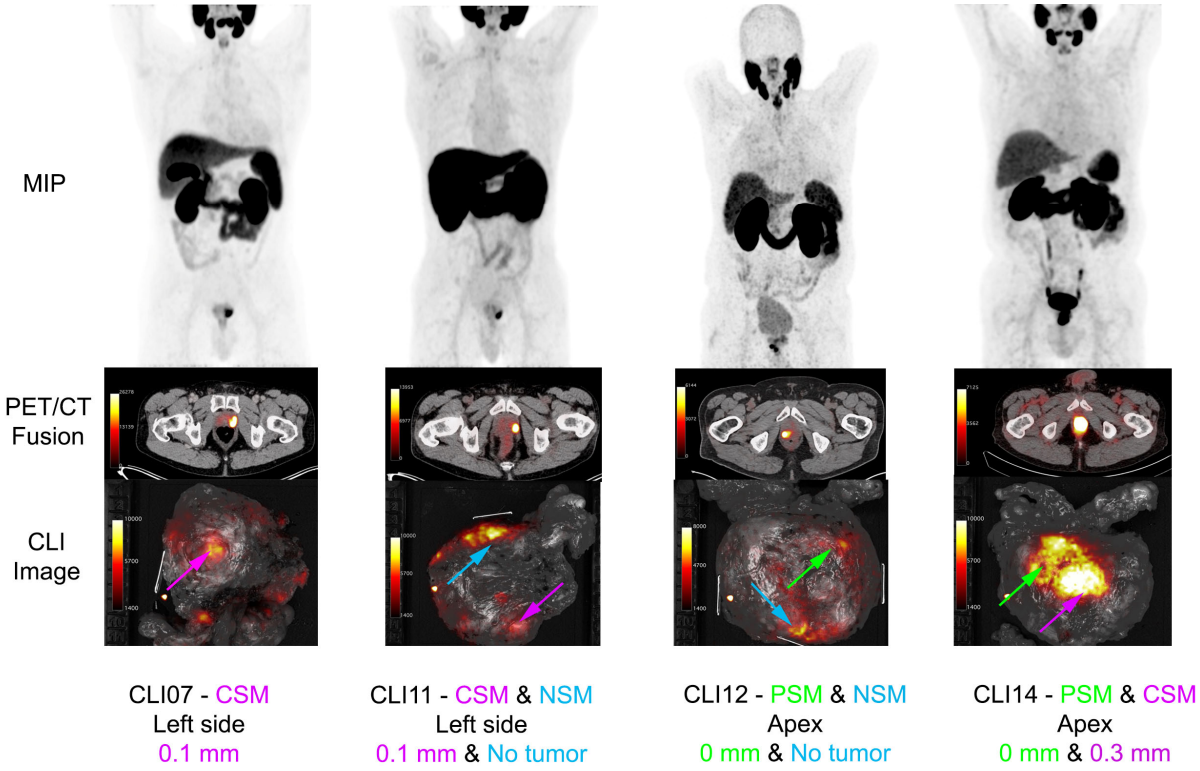

FIGURE 1. Examples of PET/CT and CLI images from four patients. Top row: maximum intensity profile (MIP) of the pre-operative PSMA PET. Second row: transversal PET/CT slide at the height of the primary tumor. Third row: CLI of excised prostate specimens without an optical filter. The arrows locate the hotspot areas, green a PSM, blue an NSM, and pink a CSM with the tumor ≤1mm from the margin, according to the pathologist. The corresponding tumor to margin distances on histopathology are noted below the images.

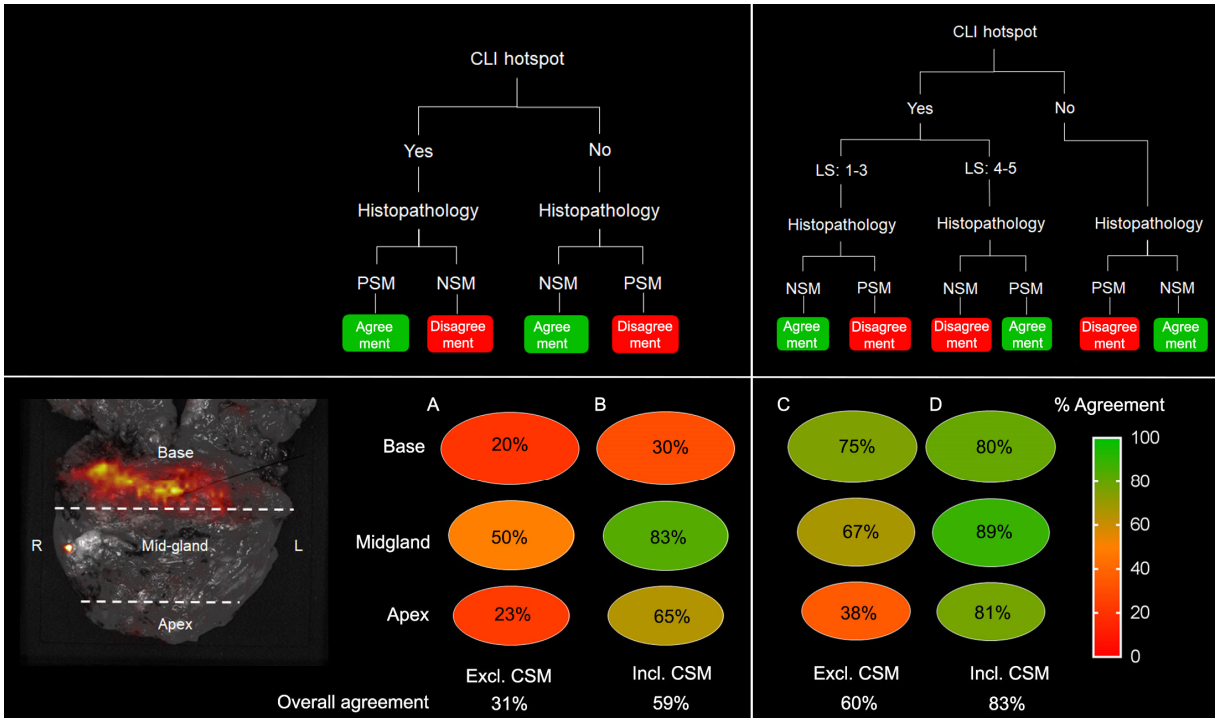

FIGURE 2. Agreement between CLI and histopathology in all patients divided in 3 regions of the prostate. A) shows the agreement between CLI hotspot (yes/no) and histopathology (PSM/NSM), excluding CSM B) the agreement includes CSM (≤1mm). C) agreement when adding a Likert score to the CLI hotspot. D) the agreement with Likert score includes CSM. Overall agreement is noted below the circles. R=right, L=left, CLI=Cerenkov luminescence imaging, NSM=negative surgical margin, PSM=positive surgical margin, CSM=close surgical margin, excl.=excluding, incl.=including.

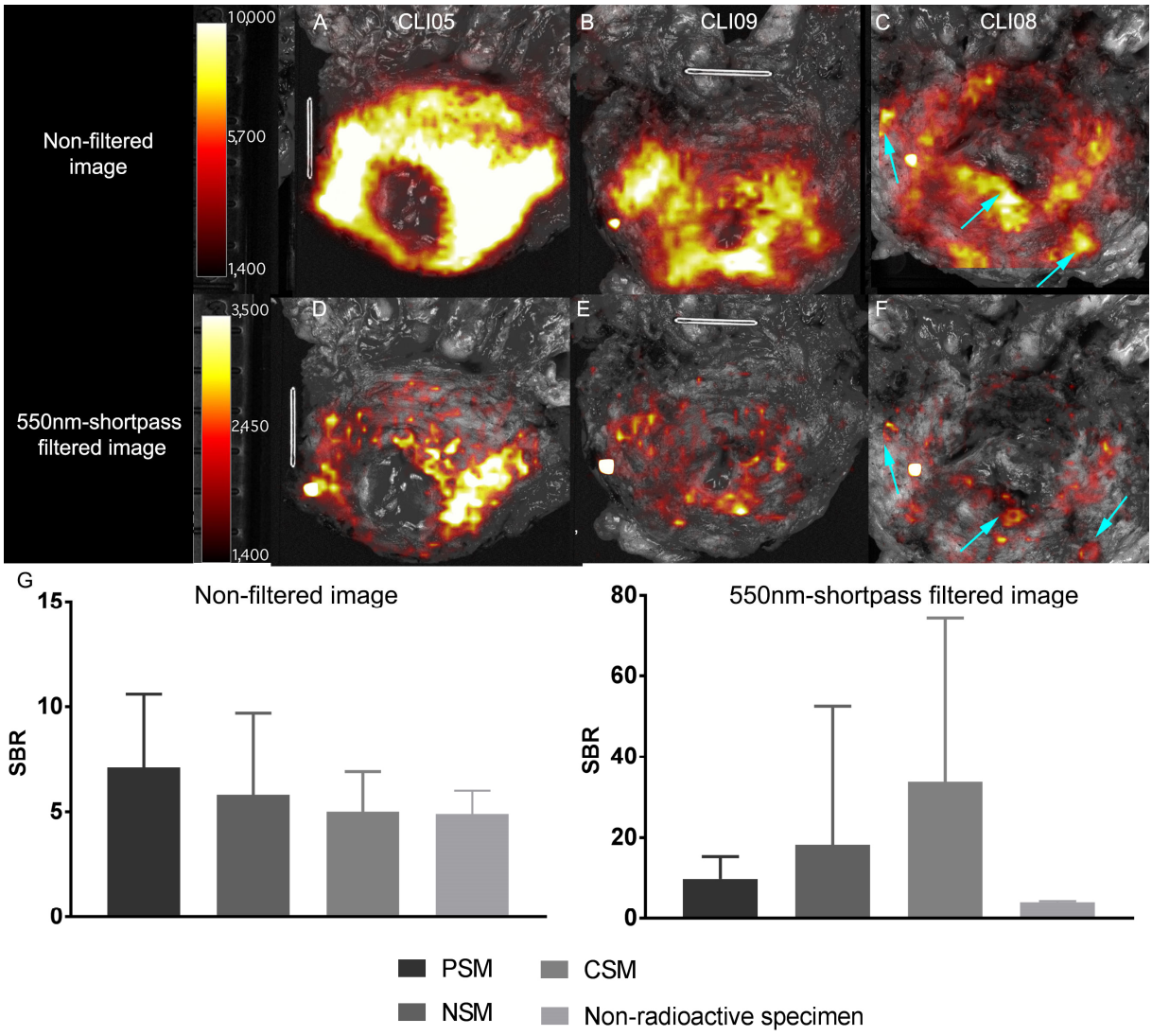

FIGURE 3. CLI images from the prostate base in ^{68}Ga-PSMA-11 patients and a bar chart showing the signal-to-background (SBR) of CLI and chemiluminescence. A and B: unfiltered images of chemiluminescence at the base. D and E: the corresponding 550nm shortpass filtered images. C and F: the base of patient 8, which had multiple PSMs at the base (see blue arrows). These images show that visual distinction between of chemiluminescence and actual PSMs is difficult. G: Bar chart displaying the SBR of chemiluminescence in non-radioactive specimens and that of PSM, NSM and CSM in patients non-filtered and filtered images. The average SBR is derived from all patient data, in which lesions on all sides of the prostate were included. Note the difference in scaling.

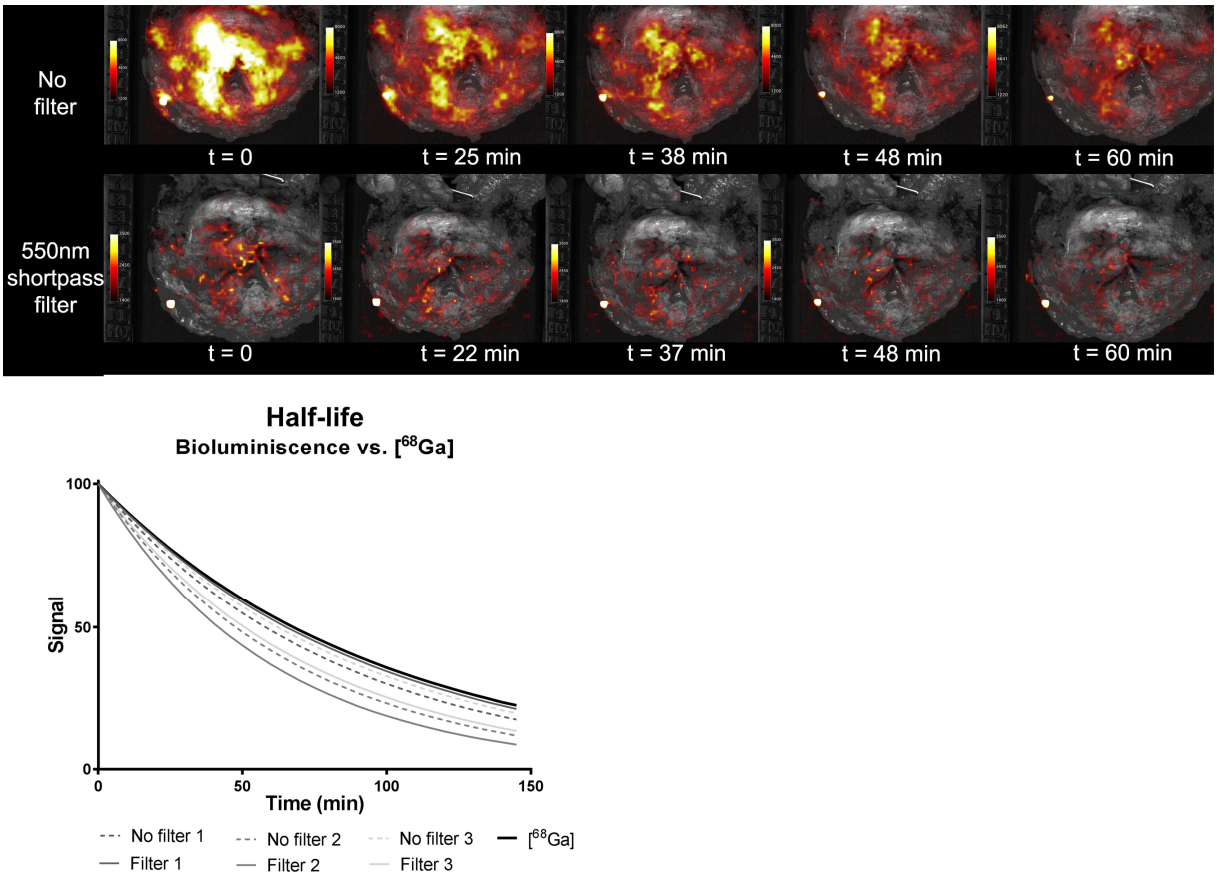

FIGURE 4. Sequential imaging of non-radioactive prostate specimens to determine the effect of time on the intensity of the chemiluminescence signal. Top row: images without filter. Bottom row: images with 550nm shortpass filter. The same scaling is used in all images. The graph displays the half-life of chemiluminescence in three non-radioactive specimens on filtered and non-filtered images, and of [^{68}Ga].

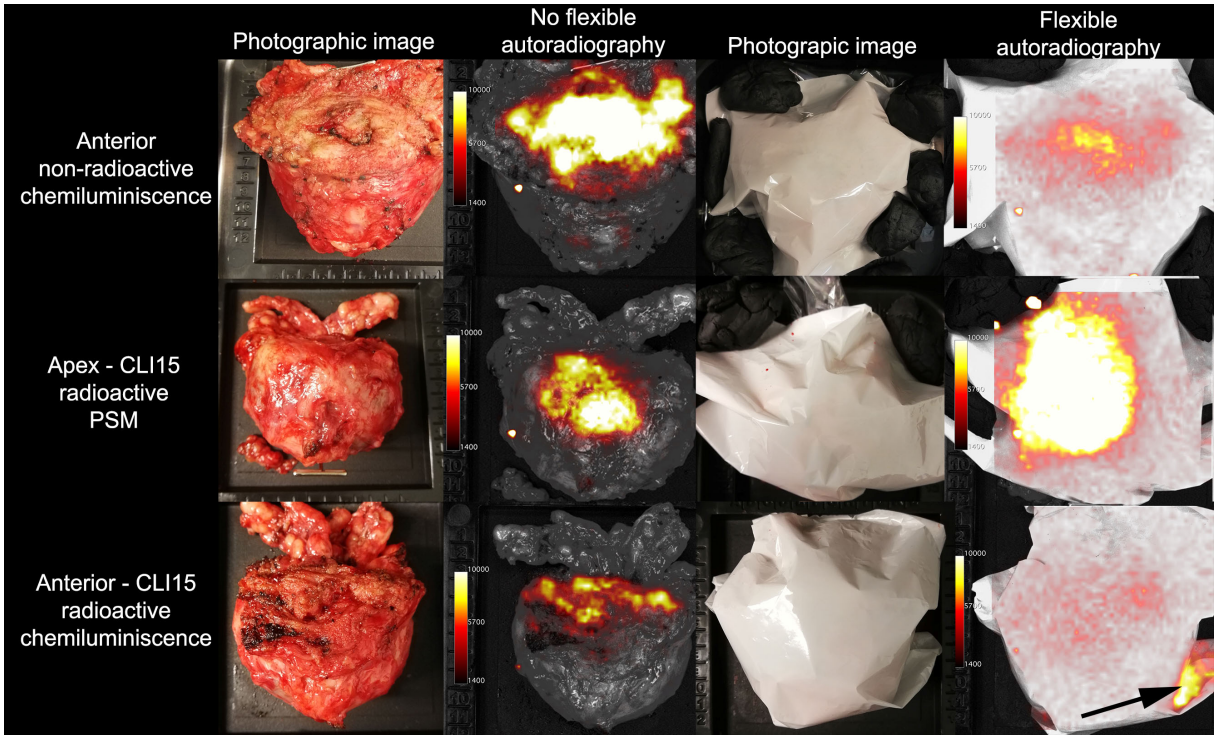

FIGURE 5. Flexible autoradiography (FAR) images of ^{68}Ga-PSMA-11 containing prostate specimens and non-radioactive prostate specimens to investigate the effect of FAR on the tumor and chemiluminescent signal levels. FAR reduced the chemiluminescence in both the non-radioactive (60%) and radioactive specimen (70%) (top and bottom row). FAR amplified the signal originating from the tumor (center row). The black arrow shows contamination of the scintillator. The same scaling is used for all images.

Graphical abstract

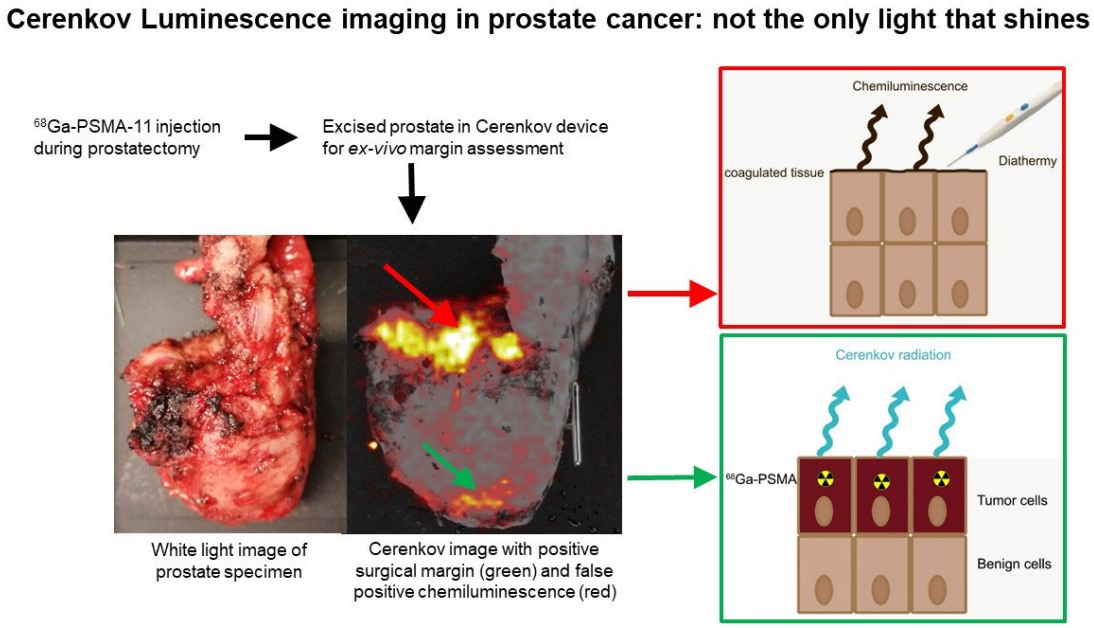

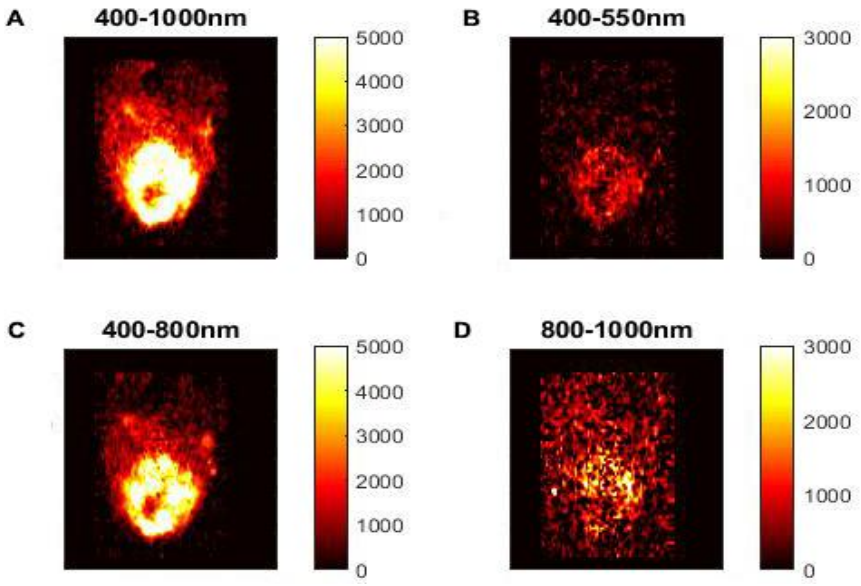

Supplemental Figure 1. Cerenkov image of the non-radioactive base imaged with an exposure time of 150s, 8x8 binning with A) no optical filter, B) a 550nm shortpass filter, C) a 800nm shortpass filter and D) the result of the subtraction of C from A, resulting in the theoretical signal present in the 800-1000nm spectrum. The signal of the filters resulted in a reduction of 87%, 20% and 80% for B, C, and D, respectively compared to the signal of the original non-filtered image (A). Thus, indicating that chemiluminescence was still present, and that differentiation using this 800nm shortpass filter in prostate specimens is not helpful for clinical decision-making.

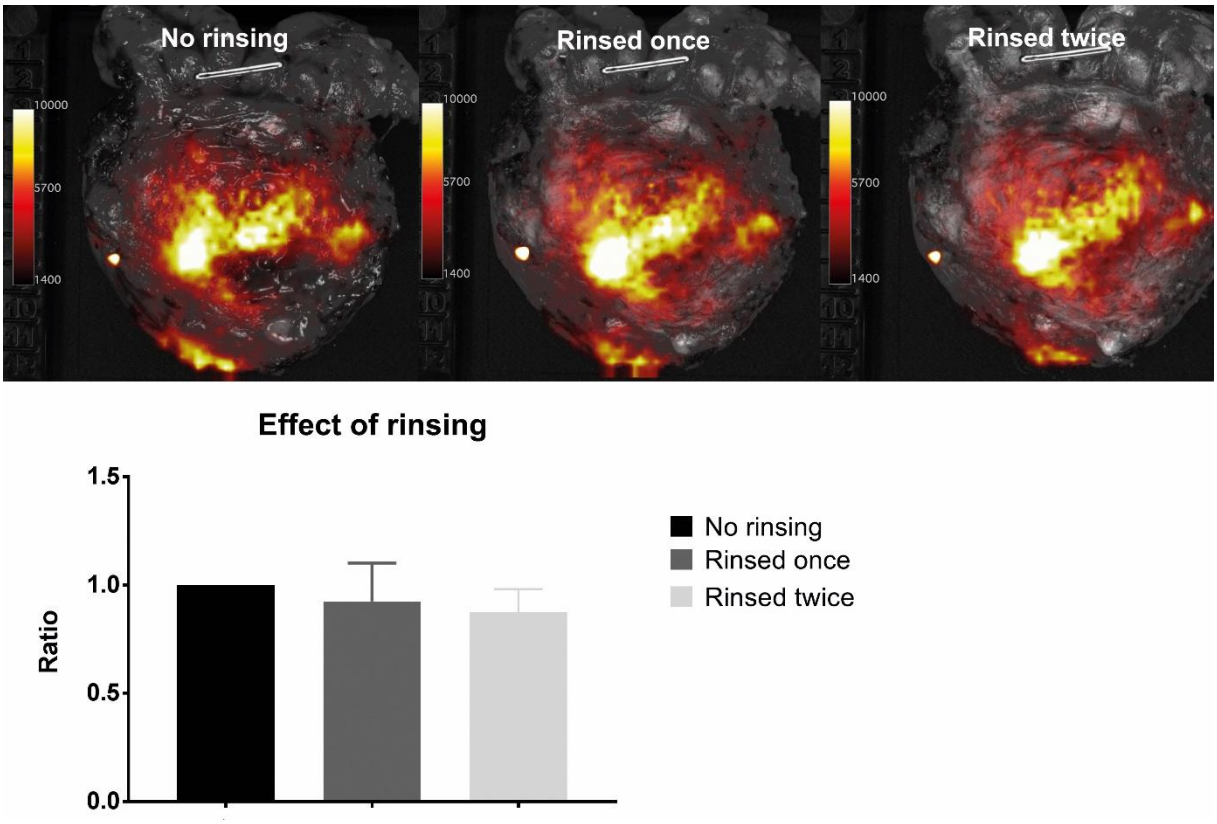

Supplemental Figure 2. Effect of rinsing the prostate on the intensity level at the prostate base. First images shows the prostate directly after removal, without additional rinsing. The second image is taken 5 minutes later, after removal of possible contamination of radioactive urine and blood by using 500mL of sodium chloride. The third images is taken again 5 minutes later after rinsing it twice with sodium chloride. Images are acquired without an optical filter and the same scaling is applied. The bar chart displays the ratio between the average intensity level after rinsing it once or twice compared to the intensity level where no rinsing is applied.

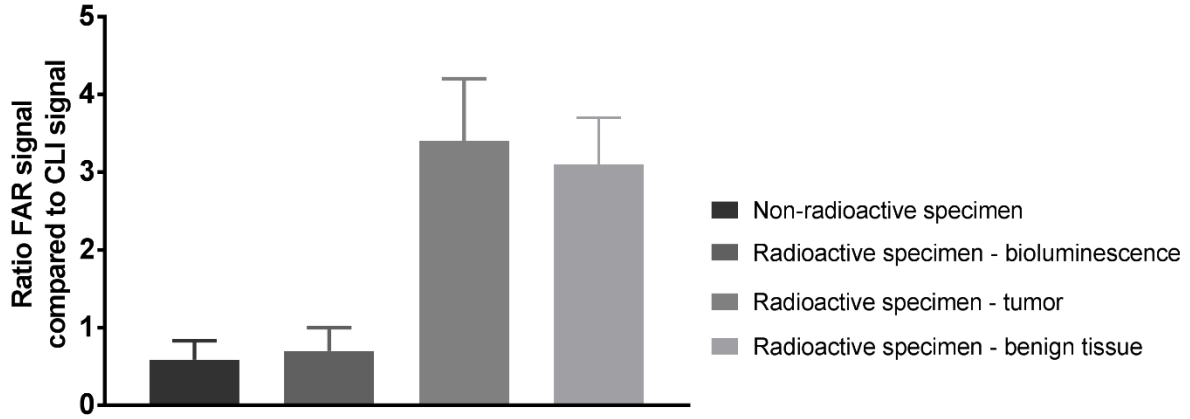

Supplemental Figure 3. A bar chart showing the effect of the application of flexible autoradiography (FAR) in different specimens. The signal is displayed as a ratio compared to the unfiltered CLI image without FAR. The FAR is applied in non-radioactive and in radioactive specimens. In the latter, the three bar charts display the signals originating from areas with tumor, benign tissue and areas where diathermy was applied. Each bar chart displays the average ratio and standard deviation measured 3 different specimens.

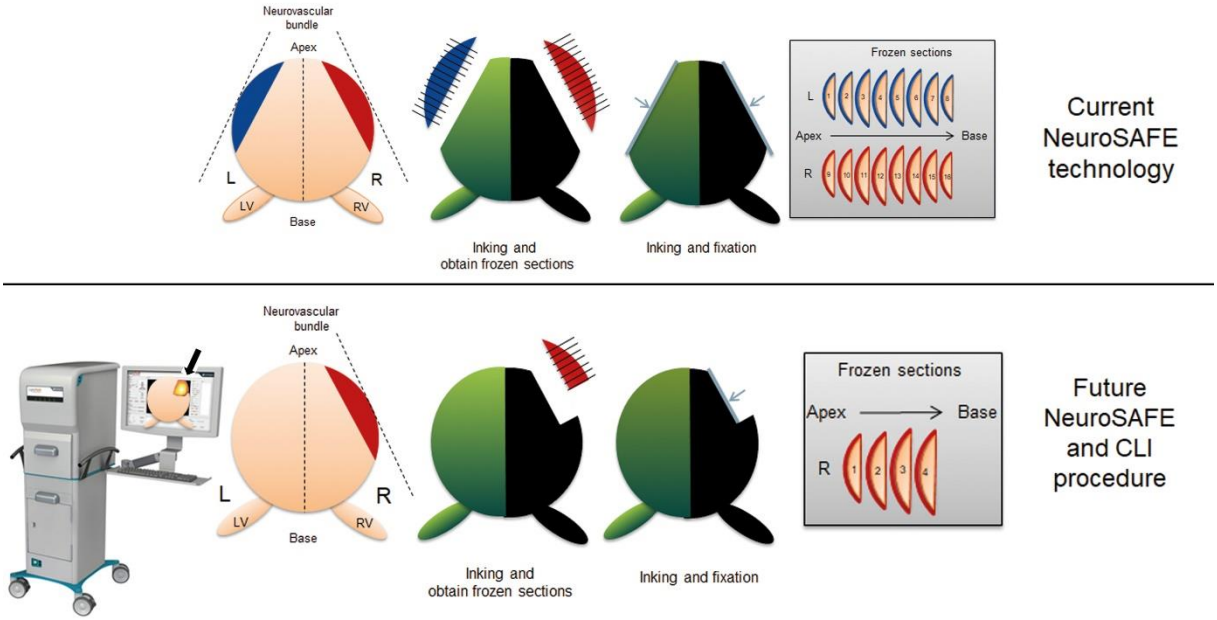

Supplemental Figure 4. Schematic overview of the current NeuroSAFE procedure (top) and potential future NeuroSAFE procedure if combined with CLI (bottom). Top: currently the neurovascular bundles are inked left (L) and right (R) in a different color. From these bundles frozen sections are obtained. The sections are assessed by a pathologist for the presences of tumor in the resection margin near the bundle. Bottom: by using the information from CLI certain areas of interest could be identified and subsequently evaluated with NeuroSAFE (see black arrow). These areas can then be inked and frozen sections obtained. By focusing only on areas at risk based on CLI, less sections need to be made and assessed by NeuroSAFE, thus making the procedure faster. As a CLI acquisition of both neurovascular bundles only takes 5 minutes.

Supplemental Table 1. Agreement between CLI and histopathology at three regions of the prostate. The regions are divided into a PSM, a CSM (tumor ≤1mm from the surface), and a NSM (tumor >1mm away from the surface) based on histopathology. CLI is divided into the presence of hotspots (yes/no) and categorized by Likert scores (1-3: likely NSM, 4-5: likely PSM). The colors of the cells represent the agreement as follows: if hotspot yes and a NSM on histopathology then there is no agreement (red), if it is a PSM on histopathology then green. Orange represents the CSM, the agreement depends on the definition: if the agreement excludes the CSM, then the CSM is counted as a NSM on histopathology. When including the CSM in the agreement, then the CSM is counted as a PSM on histopathology. The agreement between CLI and histopathology is given at every region and overall, excluding and including CSM.. LS= Likert Score, PSM= Positive surgical margin, NSM= negative surgical margin, CSM= close surgical margin, CLI= Cerenkov luminescence imaging, x= no lesions in this category.

Loca-tion	Based on Histopathology	Based on CLI				
		Hotspot yes	Hotspot no	Hotspot yes LS 1-3	Hotspot yes LS 4-5	Hotspot no
Base	NSM	14	x	15	x	x
	CSM	2	x	1	1	x
	PSM	4	x	4	x	x
	Agreement excluding CSM	4/20 =20%		15/20=75%		
	Agreement including CSM	(4+2)/20=30%		(15+1)/20=80%		
Mid-gland	NSM	3	9	1	2	9
	CSM	6	x	2	4	x
	PSM	x	x	x	x	x
	Agreement excluding CSM	9/18 =50%		(9+1+2)/18=67%		
	Agreement including CSM	(6+9)/18=83%		(9+1+2+4)/18=89%		
Apex	NSM	9	x	4	5	x
	CSM	11	x	x	11	x
	PSM	6	x	x	6	x
	Agreement excluding CSM	6/26 =23%		(6+4)/26=38%		
	Agreement including CSM	(6+11)/26=65%		(6+4+11)/26=81%		
Overall	Agreement excluding CSM	31%		60%		
	Agreement including CSM	59%		83%		